Journal of Sound and Vibration (1998) **215**(4), 743–762
Article No. sv981595

MOVEMENT OF THE UPPER-BODY OF SEATED SUBJECTS EXPOSED TO VERTICAL WHOLE-BODY VIBRATION AT THE PRINCIPAL RESONANCE FREQUENCY

Y. Matsumoto and M. J. Griffin

Human Factors Research Unit, Institute of Sound and Vibration Research, University of Southampton, Southampton SO17 1BJ, England

(*Accepted* 16 *March* 1998)

The dynamic responses of eight male subjects exposed to vertical whole-body vibration have been measured at eight locations of the body in three directions within the sagittal plane: in the vertical, fore-and-aft and pitch axes. The motions were measured on the body surface at the first, fifth and tenth thoracic vertebra (T1, T5, T10), at the first, third and fifth lumbar vertebra (L1, L3, L5) and at the pelvis (the posterior–superior iliac spine), and were corrected so as to estimate the motions of the skeleton. The head motion was measured with a bite-bar. The force at the seat surface was also measured. The subjects were exposed to vertical random vibration in the frequency range from 0·5–20 Hz at a magnitude of 1·0 ms^{-2} r.m.s. The movement of the upper-body at the principal resonance frequency of the driving-point apparent mass is illustrated by using the transmissibilities from seat vertical vibration to vertical and fore-and-aft vibration at the eight locations on the body. A bending of the lumbar spine, and probably the lowest thoracic spine, possibly coupled with a rocking motion of the upper thoracic spine about the lower thoracic spine, appeared to be dominant. A small bending along the full length of thoracic spine was also found. Pitch motion of the pelvis, possibly accompanied by longitudinal and shear deformations of the tissue underneath the pelvis, was found to occur near the resonance frequency range, but did not appear to make a principal contribution to the resonance observed in the apparent mass. Any significant axial motions along the spine occurred at higher frequencies.

1. INTRODUCTION

The dynamic responses of seated people exposed to whole-body vibration have been investigated in many studies. Various frequency response functions have often been used to represent the dynamic responses of the body. The driving-point response functions, such as the mechanical impedance and the apparent mass, which are ratios between the force and the motion at the driving-point, have been used to represent the dynamic characteristics of the body. Transmissibilities, the ratios between the motions at two distant points, represent the relative motion between two points of interest at each frequency; motion at the driving-point is usually used as the reference motion for transmissibilities.

When people are exposed to vertical whole-body vibration, one of the consistent findings is a principal resonance in frequency response functions in the frequency region of 5 Hz. A resonance of the driving-point mechanical impedance at about 5 Hz was first reported by Coermann [1] using eight subjects. Fairley and Griffin [2] found a main resonance at about 5 Hz in the driving-point apparent masses of 60 people. The transmissibilities of

0022–460X/98/340743 + 20 $30.00/0

vertical vibration from the seat to various parts of the seated body, such as to the spine, also show a peak at almost the same frequency as the peak in the driving-point responses in previous studies (e.g. those of Panjabi *et al*. [3], and Pope *et al*. [4]).

The principal resonance of the seated body at about 5 Hz has been previously suggested to be associated with some dynamic mechanisms of the body. Hagena *et al*. [5] measured the dynamic response of both standing and seated subjects at the head, the seventh cervical vertebra, the sixth thoracic vertebra, the first, fourth and fifth lumbar vertebra and the sacrum. Comparing the vertical transmissibilities from the vibrator platform vibration to each measurement location with those from the sacrum to each upper location, they concluded that the resonance observed at around 4 and 5 Hz corresponded to motion of the entire body, while the second resonance between 7 and 10 Hz represented motion of the spinal column. Sandover and Dupuis [6] reanalyzed film of the motion of the lower spine as investigated by Christ and Dupuis [7] and hypothesized that the resonances at about 4 Hz observed during human response to vertical vibration were related to bending in the lumbar spine and possibly a rocking motion of the pelvis. Bending motion of the lumbar spine was also suggested by Hinz *et al*. [8]. They stated that the relative vertical accelerations between L3 and L4 found at 4·5 Hz were mainly caused by bending of the spine. It was also stated that the time relations between extreme accelerations at the lumbar vertebrae and those at the head and the acromion indicated that the vertical motion of the body parts above L3, rather than a pitching of the pelvis which might be a secondary effect, caused a bending of the lumbar spine. Pope *et al*. [4] suggested that the first natural frequency of the vertical transmissibility to the third lumbar vertebra is "due primarily to a vertical response of the buttocks-pelvis system" . . . "to compression of the buttocks tissue and the interaction of this vertical response with the rotational subsystem".

Kitazaki and Griffin [9] investigated vibration modes of the seated body in the mid-sagittal plane at frequencies below 10 Hz using experimental modal analysis. They extracted a total of eight vibration modes in which acceleration responses of the spine (i.e., at the first, sixth and eleventh thoracic vertebrae, the third lumbar vertebra, and the sacrum), of the pelvis, viscera and the head to whole-body vertical vibration were measured. The fourth mode they obtained, at 4·9 Hz, was found to be a combination of an entire body mode with vertical and fore-and-aft pelvis motion, due to buttocks tissue deformation, in phase with a vertical visceral mode, and a bending of the upper thoracic and cervical spines. The fifth mode at 5·6 Hz appeared to contain a bending mode of the lumbar spine and the lower thoracic spine and a motion of the head which might have been pitch motion. A rotational mode of the pelvis was contained in the sixth mode at 8·1 Hz and the seventh mode at 8·7 Hz. The authors also conducted a study of vibration modes of the seated body using the finite element method [10]. A two-dimensional model was developed by comparison of the vibration mode shapes with those extracted from experimental data [9]. A total of seven modes was obtained from the mathematical model. It was concluded that the principal resonance of the driving point response at about 5 Hz consisted of an entire body mode, in which the head, spinal column and the pelvis move together, with vertical and fore-and-aft pelvic motion due to deformation of tissue beneath the pelvis occurring in phase with a vertical visceral mode, which was the fourth mode at 5·06 Hz. A bending mode of the entire spine was found in the fifth mode at 5·77 Hz which was stated to make a minor contribution to the principal resonance. As in the experimental result, a pelvis rotation was found in both the sixth mode (at 7·51 Hz) and in the seventh mode (at 8·96 Hz).

The objectives of the present study were: (i) to measure the dynamic responses of seated people at locations on the upper-body, using different measurements from those obtained by Kitazaki and Griffin [9], so as to define the form of body movements during exposure to vertical whole-body vibration, and (ii) to identify the mechanism contributing to the principal resonance seen in the apparent mass of the seated body.

2. EXPERIMENTAL METHOD

Eight male volunteers, aged from 22–33 yrs, took part in an experiment. The ranges of their height and weight were from 1·66–1·81 m and 63–83 kg, respectively. They were seated on a flat rigid seat which was mounted on a 1-metre stroke electrohydraulic shaker. A computer generated random signal, which was common for all subjects, was fed into the shaker which produced a random vertical vibration having a flat constant bandwidth acceleration spectrum over the frequency range 0·5–20 Hz. The duration and magnitude of the vibration were 60 s and $1{\cdot}0\ \mathrm{ms}^{-2}$ r.m.s., respectively. A force platform, Kistler 9281B, was secured to a flat rigid seat which was mounted onto the shaker platform to measure the force at the interface between seat and subjects. The acceleration at the seat surface was also measured at the centre of the top plate of the force platform with a piezoresistive accelerometer (Entran EGCS-DO-10). The posture of subjects was a "normal sitting posture" defined as sitting looking straight ahead and with the upper body in a comfortable and upright posture without backrest. Subjects were asked to avoid any voluntary movements. No foot rest was used: the feet were allowed to hang freely.

The motion of the body was measured at eight locations: at the head, six points along the spine (the first, fifth and tenth thoracic vertebrae, and the first, third and fifth lumbar vertebrae: T1, T5, T10, L1, L3, L5) and the pelvis (on the posterior–superior iliac spine of the right ilium 50 mm away from the mid sagittal plane). A bite-bar in which three translational accelerometers (Entran EGA-125(F)*-10D and EGAX-F-5) were installed was used for measuring the head motion in the vertical, fore-and-aft and pitch directions (see reference [11]). The separation between two accelerometers measuring the vertical motions for calculation of the pitch motion of the head was 115 mm.

The motions of the vertebrae and the pelvis were measured with accelerometers attached to the body surface. As suggested by Hinz *et al*. [8] and Sandover and Dupuis [6], potential pitch motion of the vertebrae has an effect on the measurement of translational motions at the body surface (i.e., those at the centre of the vertebral bodies could be different from those at the spinous processes). Therefore, the vertebral motions in the vertical, fore-and-aft and pitch axes were measured at the body surface such that the motions at the centres of the vertebral bodies could be estimated. Sets of two miniature accelerometers (either Entran EGA-125(F)*-10D or EGAX-F-5) were attached to T-shaped blocks of

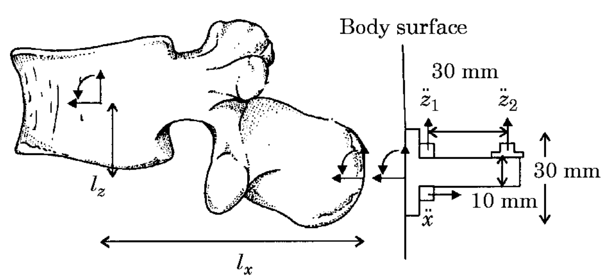

Figure 1. Measurements over a vertebra showing the T-shaped balsa block and miniature accelerometers. (Transmissibilities to the centre of the vertebra were estimated from those to the spinous process obtained from surface measurement.)

Table 1

Horizontal and vertical distances between the centres of the vertebral bodies and the tips of the spinous processes, used in the estimation of the transmissibilities to the centres of the vertebral bodies

Location	Horizontal (mm)	Vertical (mm)
T1	50	10
T5	50	30
T10	55	15
L1	60	10
L3	65	10
L5	60	15

balsa wood with a separation of 30 mm so as to measure both the vertical and pitch motions at the body surface over the spine and the pelvis (see Figure 1). The fore-and-aft motion was also measured with another miniature accelerometer attached to a different face of the block. The weight of the block, including the accelerometers and their cables, was about 4 g. The block was attached to the body surface by double-sided adhesive tape and adhesive plaster with a contact area of 20 mm (horizontal) by 30 mm (vertical). Signals from all the accelerometers and the force platform were acquired at 128 samples per second after low-pass filtering at 20 Hz.

Pope *et al*. [12] showed that a motion measured on the body surface over a bone may be modified by the tissue and skin between the bone and the transducer. Accordingly, a data correction method for surface measurements, developed by Kitazaki and Griffin [13] was applied, in which it is assumed that the local dynamic system consisting of the tissue and the accelerometer could be analogized with a single degree-of-freedom linear system. The natural frequency and damping ratio of the local tissue–accelerometer system at each measurement location and in each direction was derived from the response to free damped oscillation tests performed before vibration exposure. The correction method made it possible to obtain the motions at the spinous processes from those measured on the body surface.

The locations of all measurement sites were measured. The vertical location (in the z-axis) was the height of each point above the seat surface. The horizontal location (in the x-axis) was the distance between the body surface at the measurement point and a reference vertical surface fixed to the rear of the seat. The positions of vertebrae were then estimated using distances between the centres of the vertebral bodies and the tips of the spinous processes using the values shown in section 3 in Table 1. The thickness of the tissue between the body surface and the spinous processes was neglected. The location of the head (the mouth) and the pelvis (the posterior–superior iliac spine) and the estimated centres of the vertebral bodies as measured for each subject are shown in Appendix 1.

3. ANALYSIS

In the analysis, upward and forward motions were taken as positive vertical (z-axis) and fore-and-aft (x-axis) motions, respectively, as defined in ISO 2631 [14]. Pitch motions which rotated clockwise when looked at from the right hand side of the body were taken as positive.

The apparent mass, $M(f)$, was calculated by dividing the cross spectral density function between the seat acceleration and the resulting force at the seat surface, $S_{sf}(f)$, by the power spectral density function of the seat acceleration, $S_s(f)$:

$$M(f) = S_{sf}(f)/S_s(f). \quad (1)$$

The transmissibilities, $T(f)$, were also obtained by using the cross-spectral density method, with the seat acceleration used as a reference:

$$T(f) = S_{sb}(f)/S_s(f). \quad (2)$$

Here $S_{sb}(f)$ is the cross-spectral density between the acceleration at the seat and that measured at a location of the body. A resolution of 0·25 Hz was used for the calculation, which gives 60 degrees-of-freedom corresponding to accuracy and confidence levels of about 80% at ± 1 dB.

Accelerations in the z-axis obtained from accelerometers attached to a balsa block near the body surface, $\ddot{z}_1$ in Figure 1, were regarded as those along the body surface on the assumption that the distance between the body surface and the accelerometers, 5 mm, could be neglected. Those from the accelerometers on a different face of the block were regarded as being normal to the surface ($\ddot{x}$ in Figure 1). Pitch motion was obtained by dividing the difference between the two vertical accelerations ($\ddot{z}_1$ and $\ddot{z}_2$ in Figure 1) by the distance between two accelerometers (i.e., 30 mm). It was assumed that both the bite-bar and balsa blocks were rigid in the frequency range used in the experiment.

The transmissibilities to each location and in each axis were corrected to reduce the discrepancy between the motion of the skeleton and that measured at the body surface [13],

$$T_b(f) = C(f)T_s(f), \quad (3)$$

where $T_b(f)$ and $T_s(f)$ are the transmissibilities to the bone and to the surface over the bone, respectively, expressed in complex numbers. The values of the correction frequency functions, $C(f)$, were determined from the natural frequencies and the damping ratios of the local tissue–accelerometer systems obtained from free oscillation tests,

$$C(f) = [1 - (f/f_0)^2 + 2i\zeta(f/f_0)]/[1 + 2i\zeta(f/f_0)], \quad (4)$$

where f_0 and ζ are the natural frequency and the damping ratio of the local system, respectively, and $i^2 = -1$.

The effect of the inclination of the body surface on the measurement was reduced by using the angle of the surface relative to the vertical axis. This effect was particularly significant at T1 where the angle of the surface to the vertical varied between 20 and 35 degrees among the eight subjects. The corrected transmissibilities to the spinous processes along the body surface, $T_{z1}(f)$, and normal to the surface, $T_{x1}(f)$, expressed in complex numbers were compensated linearly by the angle between the body surface and the vertical axis, θ, in the frequency domain,

$$T_x(f) = T_{x1}(f)\cos\theta + T_{z1}(f)\sin\theta, \qquad T_z(f) = -T_{x1}(f)\sin\theta + T_{z1}(f)\cos\theta, \quad (5, 6)$$

where $T_x(f)$ and $T_z(f)$ are the required transmissibilities in the x-axis (i.e., fore-and-aft) and the z-axis (i.e., vertical) in an earth-based co-ordinate system. The pitch displacements at each measurement point were assumed to be small so that the angle of the surface did not change during exposure. This was a reasonable assumption according to the results presented below. For example, this correction reduced the fore-and-aft transmissibility to T1 of a subject from about 0·6 to about 0·1 at the lowest frequencies (e.g., about 0·5 Hz), agreeing with the expectation that the body would mainly move in the vertical direction at low frequencies.

As mentioned above, if there is pitch motion of the vertebrae, transmissibilities to the spinous processes will be different from those to the centres of the vertebral bodies. Therefore, assuming that the vertebrae were rigid and that their velocities in the pitch direction were small, transmissibilities to the centres of the vertebral bodies were estimated using those determined for the spinous processes for the three directions within the sagittal plane,

$$T_{xc}(f) = T_{xs}(f) + l_z T_{ps}(f), \qquad T_{zc}(f) = T_{zs}(f) - l_x T_{ps}(f), \tag{7, 8}$$

where $T(f)$ is the complex transmissibility and the subscripts x, z and p represent the vertical, fore-and-aft and pitch directions, respectively. The subscripts c and s represent the centres of the vertebral bodies and the spinous processes, respectively. The assumed horizontal and vertical distances, l_x and l_z, between the centres of the vertebral bodies and the tips of the spinous processes are given in Table 1 (see Figure 1).

The transmissibilities in the vertical and fore-and-aft axes, obtained by the method explained above, were used to determine the movement of the upper-body at the principal resonance frequency determined from the apparent mass for each subject. Using the moduli and the phases of the transmissibilities at the resonance frequency, the position of each measurement point in the sagittal plane was calculated,

$$x_j = x_{0j} + T_{xj} A \sin(2\pi f_r t + \phi_x), \qquad z_j = z_{0j} + T_{zj} A \sin(2\pi f_r t + \phi_z), \tag{9, 10}$$

where j indicates the position of the measurement point, and x and z are the horizontal and vertical components in the co-ordinate defined in Appendix 1, respectively. The values of x_0 and z_0 represent the initial position of the measurement point, j, as given in Appendix 1; f_r is the principal resonance frequency determined from the apparent mass; T_x and ϕ_x are the modulus and the phase of the fore-and-aft transmissibility at f_r; T_z and ϕ_z are the modulus and the phase of the vertical transmissibility at f_r; A is the amplitude of the vertical displacement of the reference motion (i.e., the seat surface displacement) at the frequency f_r; t is the time.

4. RESULTS

As reported in previous studies, the apparent masses of the subjects showed a clear peak in the frequency range between 4·75 and 5·75 Hz (see Figure 2). The frequencies at which the apparent masses had a principal peak are listed in Table 2. The frequencies at which the apparent mass was greatest were assumed to be the principal resonance frequencies of the subjects and are referred to as the principal resonance frequencies of the apparent mass in this study.

In a preliminary experiment a significant variability in measured vertebral pitch motion was found at frequencies above about 10 Hz when using different sizes of balsa blocks (see Figure 3). It was concluded that the estimated transmissibilities to the centres of the vertebrae were reliable in the frequency range below 10 Hz.

It was found that the pitch motions of the vertebrae resulted in up to about 20% difference in transmissibility to the vertebral bodies compared to the transmissibility to the spinous processes around 5 Hz, which agreed with the observation by Sandover and Dupuis [6]. Figure 4 illustrates the transmissibility to the spinous process, after correction by equations (3) to (6), and the transmissibility to the centre of the vertebra obtained by using equations (7) and (8), at L3 of a subject, together with the pitch transmissibility. The median estimated transmissibility to the centre of the vertebral body of L3 was compared with the transmissibilities to L3 and the vicinity reported in previous studies [3, 4, 6, 15] (see Figure 5). The median transmissibility obtained in this study was found to be similar

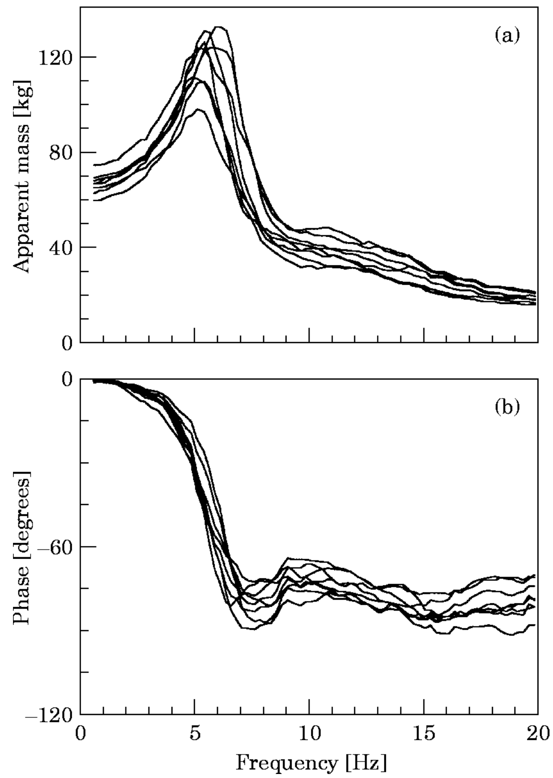

Figure 2. Apparent masses and phases of the eight subjects.

to measurements obtained with transducers mounted on pins directly threaded into the spinous processes [3, 4, 15]. The difference between the present study and the previous studies may be partly attributed to the difference in transmissibility between the centre of the vertebral body and the spinous process.

The transmissibilities between the vertical seat motion to the vertical motions at the head (i.e., the mouth), the centre of each vertebral body and the pelvis (i.e., the posterior–superior iliac spine) for eight subjects are shown in Figure 6. The variability between subjects, inter-subject variability, was large for the head, and for transmissibilities to L3 and L5 and to the pelvis at frequencies above about 7 Hz. Most vertical transmissibilities, apart from some to the head, show a peak in the frequency region of the principal resonance frequency of the apparent mass of each subject ($\pm 0{\cdot}5$ Hz). The vertical transmissibility at the principal resonance frequency tended to decrease at higher measurement locations, although this was not the case for those to T1 for which the head motion might have had an effect. The maximum transmissibility to the lumbar spine was found at the resonance frequency for six of the eight subjects. The vertical transmissibilities to L5 and to the pelvis of seven subjects show another peak between 7 and about 10 Hz,

TABLE 2

Principal peak frequencies in the apparent masses of the eight subjects

Subject	1	2	3	4	5	6	7	8
Frequency (Hz)	5·25	5·00	5·75	5·25	5·00	5·75	5·25	4·75

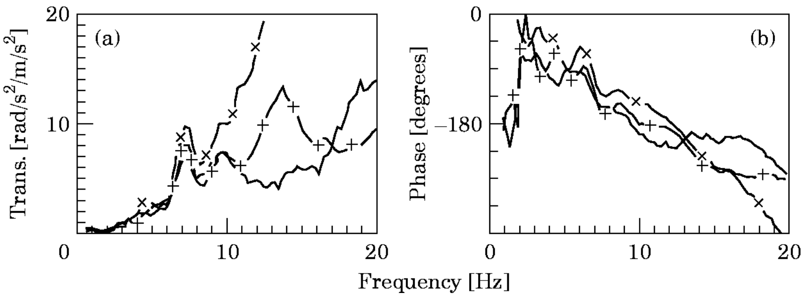

Figure 3. Pitch transmissibility to L3 measured with three T-shaped balsa blocks having different sizes: —+—, 25 mm of separation between two accelerometers; ——, 30 mm of separation; —×—, 35 mm of separation. (Results of a pilot experiment).

which had a greater magnitude than that at about 5 Hz for some subjects. This second peak was also visible in the vertical transmissibilities to the upper locations over the lumbar spine, although this was not as clear as in those to L5 and to the pelvis.

Figure 7 shows the fore-and-aft transmissibilities to each location for eight subjects. It was clear that the fore-and-aft transmissibilities to all locations, except to the head and T1, were much smaller than those in the vertical direction, as expected. The fore-and-aft transmissibilities to the head and T1 showed a peak between 6 and 7 Hz for most subjects, which was slightly higher than the principal resonance frequency of the apparent mass. The peak at this frequency range was not clear at the other locations. The fore-and-aft

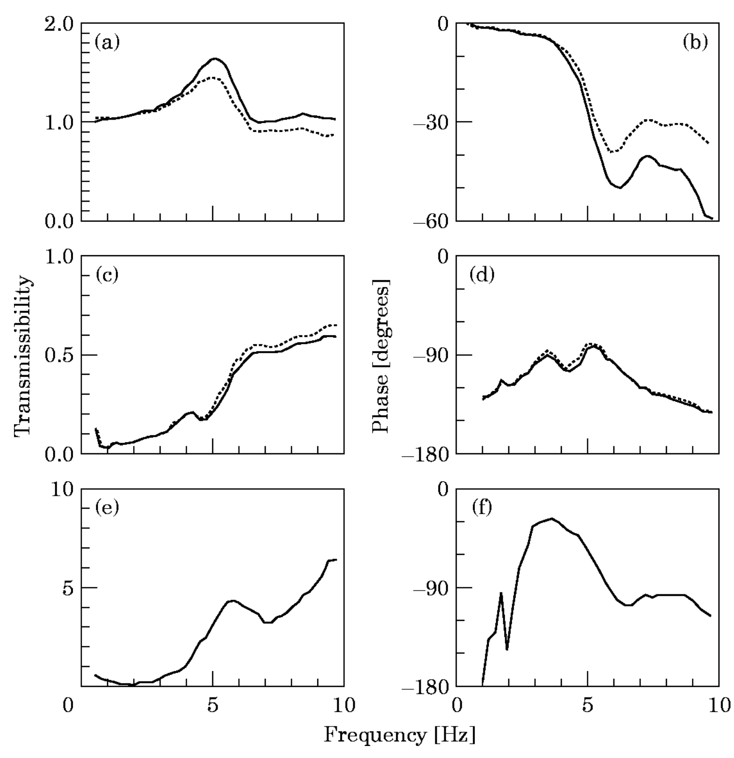

Figure 4. Transmissibilities and phases to the spinous process and to the centre of the vertebra at L3 in the vertical direction, (a) and (b), and in the fore-and-aft direction, (c) and (d), together with those in the pitch direction, (e) and (f). Key: ——, spinous process; ·····, centre of vertebra.

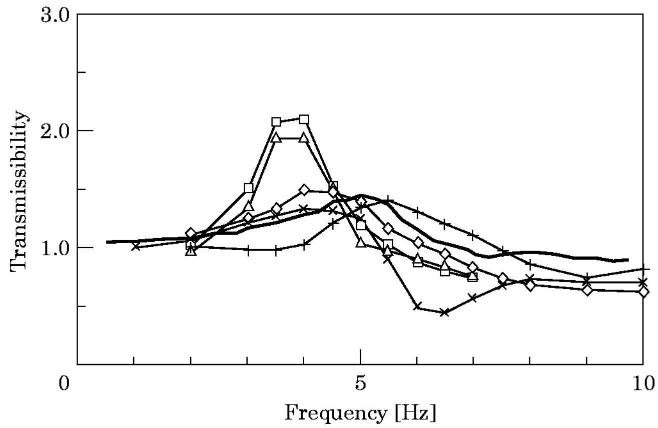

Figure 5. Comparison of the median estimated transmissibility to the centre of the vertebral body of L3, to the transmissibilities to L3, and to this vicinity reported in previous studies. (Median of five subjects from Panjabi *et al*. [3], data from one subject from Sandover and Dupuis [6] and Pope *et al*. [4], and median of three subjects from Magnusson *et al*. [15]). Key: —◇—, Panjabi *et al*. [2], L1 and L3; —□—, Sandover and Dupuis [6], L4; —△—, Sandover and Dupuis [6], L2; —×—, Pope *et al*. [4], L3; —+—, Magnussen *et al*. [15], L4; ▬▬, this study, L3.

transmissibilities to T5 and L5 tended to be smaller than to the other locations over the spine. The fore-and-aft transmissibility at the principal resonance frequency tended to increase as the measurement location was higher: the modulus was a maximum at T1 and a minimum at L5 for seven subjects. However, the modulus at T5 was smaller than at T10, the next lower point, for seven of the eight subjects.

The transmissibilities from the vertical seat vibration to the pitch motion at each location are shown in Figure 8. Although inter-subject variability was large at some locations, it was possible to find overall trends for the subjects. Most pitch transmissibilities to locations over the spine were very small below 4 Hz and increased with an increase in the frequency above 4 Hz. The pitch transmissibilities to T1 and to the heads of all subjects showed a clear peak between 5 and 7 Hz. The magnitudes of the peaks seen at the head were greater than those at T1 for seven subjects ($p < 0{\cdot}05$). The pitch transmissibilities to the locations over the spine were smaller than those to the head and T1 at frequencies below 10 Hz. At the principal resonance frequency of the apparent mass, the greatest pitch transmissibility was to the head for seven of the subjects, while pitch transmissibility to T1 tended to be greater than that of the other locations over the spine. In the region of the spine between T10 and L3, the pitch transmissibility was less than at other measurement points.

The vertical and fore-and-aft transmissibilities were used to illustrate the movement of the upper-body at the principal resonance frequency of the apparent mass for each subject, using equations (9) and (10). The moduli and phases of the transmissibilities at the resonance frequencies of all subjects that were used to illustrate the movement are shown in Appendix 2. The vertical transmissibility was greatest at the pelvis at the resonance frequency for seven subjects, of whom six showed the maximum transmissibility within the spine in the lumbar region. The phase difference of the vertical motion with respect to the seat motion tended to increase at T1 compared to those at other locations on the spine. The fore-and-aft motion at T1, where the motion was the greatest in this direction, was almost out of phase with the fore-and-aft motions at T10, L1 and L3. The fore-and-aft transmissibility to T5 tended to be smaller than at the adjacent measurement points, T1 and T10. At L5, the fore-and-aft transmissibility was the smallest for five subjects.

Figures 9 and 10 show a cycle of the movement of the all measurement points on the upper-body, using subjects 5 and 7 as examples, at the principal resonance frequencies of 5·0 Hz and 5·25 Hz, respectively. The body was viewed from the right side. In the figures, a cycle is divided into eight equal intervals such that: (a) $t = 0$, the seat surface is at the initial position; (c) $t = T/4$ (where T is the period of the seat vibration), the seat is at the highest position; (e) $t = T/2$, the seat has returned to the initial position; (g) $t = 3T/4$, the seat is at the lowest position. For illustration, the displacement of the seat surface vibration, A in equations (9) and (10), was 0·05 m: i.e., the movements shown in Figures 9 and 10 are exaggerated. At their principal resonance frequency, the movements of the upper-bodies of the other subjects, except subject 2, demonstrated consistent trends with those shown in Figures 9 and 10.

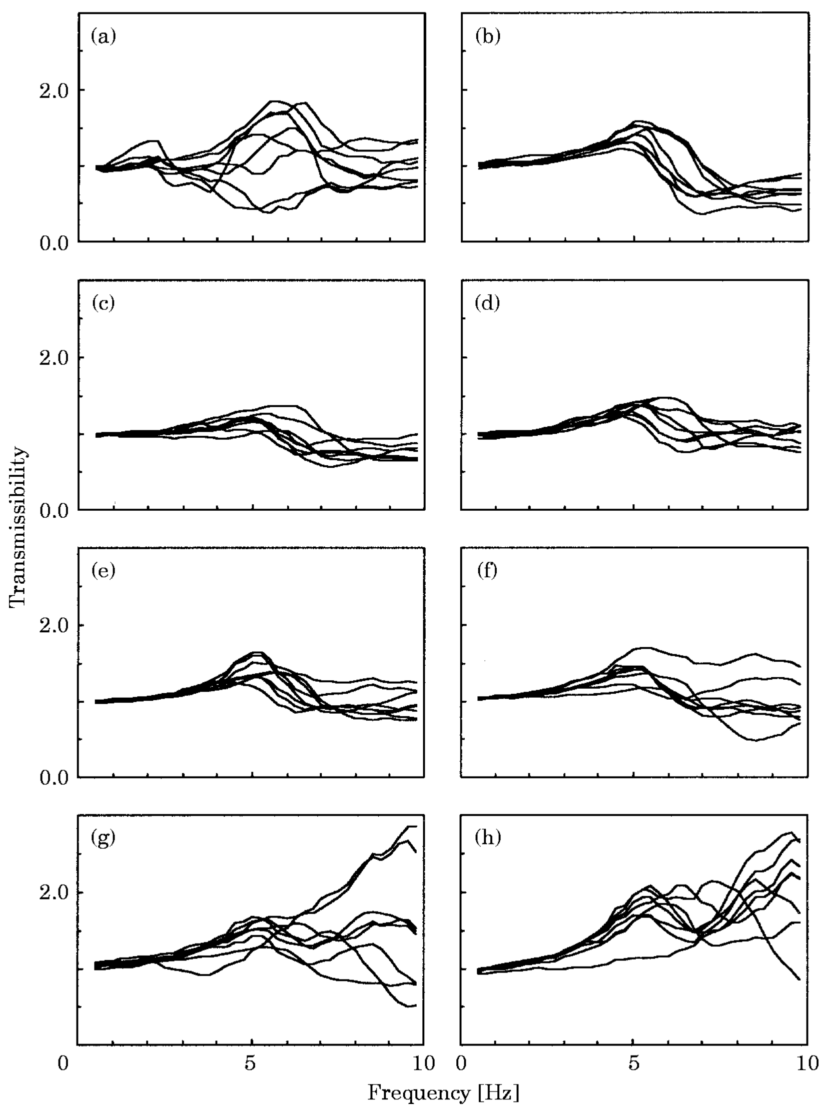

Figure 6. Vertical transmissibilities to each measurement location for the eight subjects: (a) head; (b) T1; (c) T5; (d) T10; (e) L1; (f) L3; (g) L5; (h) pelvis.

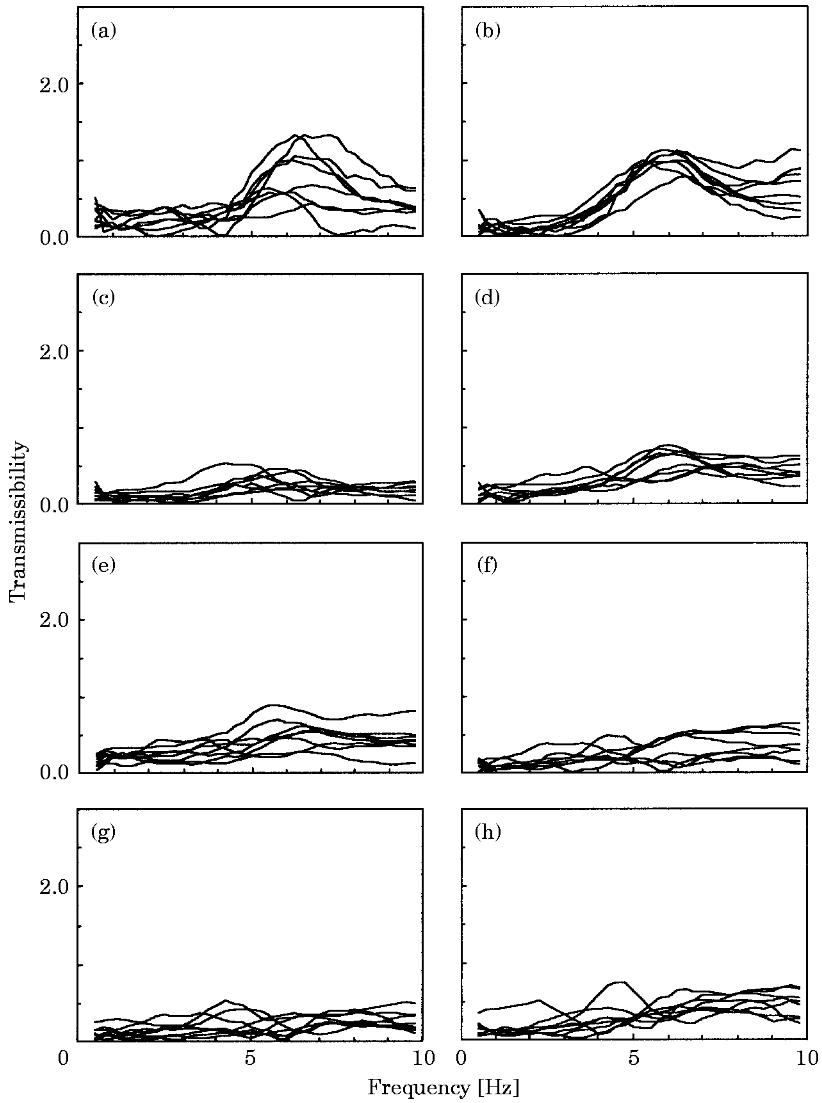

Figure 7. Fore-and-aft transmissibilities to each measurement location for the eight subjects. Part locations as for Figure 6.

It was clear that relative motion occurred between locations over the spine at the principal resonance frequency: all measurement points did not move in the same manner. Bending or rocking motions of the spine appeared to be dominant at frequencies around the resonance of the apparent mass. The upper thoracic spine, between T1 and T10, tended to rock about a point on the lower thoracic spine in the sagittal plane, with some slight bending. In the lower thoracic spine and the lumbar spine region, bending motion along the spine was more significant than in the upper thoracic spine. It seems that some pitch motion of the pelvis occurred at this frequency, although the pitch resonance of the pelvis is at a higher frequency. There was also pitch motion of the head at the principal resonance of the body.

To visualize the motions mentioned above, consider the movement of the upper-body when the seat moved upward (see Figures 9 and 10). The upper thoracic spine rocked backward, with a slight extension along the full length of the upper part of thoracic spine, while the head pitched forward. This combined movement was delayed compared to the upward seat motion, although the backward rocking was almost in phase with the extension. The pitch motion of the head was delayed compared to the rocking motion of the upper thoracic spine. The lower spine extended with upward seat motion, with a slightly smaller delay than that of the motion in the upper thoracic region. The extension of the lumbar spine possibly caused the forward motion of the upper lumbar spine and the lower thoracic spine, which may have contributed to the backward rocking motion of the upper thoracic spine. The pelvis pitched forward as the seat moved upward, although there appeared to be a delay with respect to the upward seat motion.

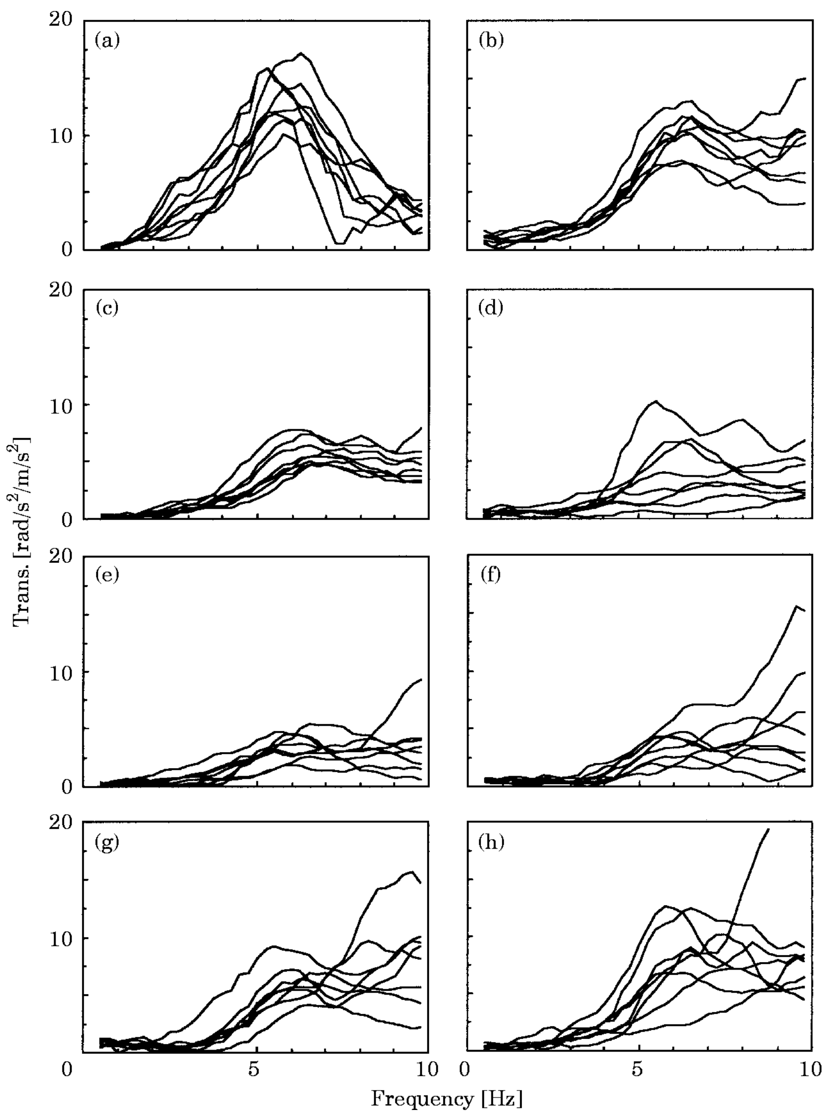

Figure 8. Pitch transmissibilities to each measurement location for the eight subjects. Part Locations as for Figure 6.

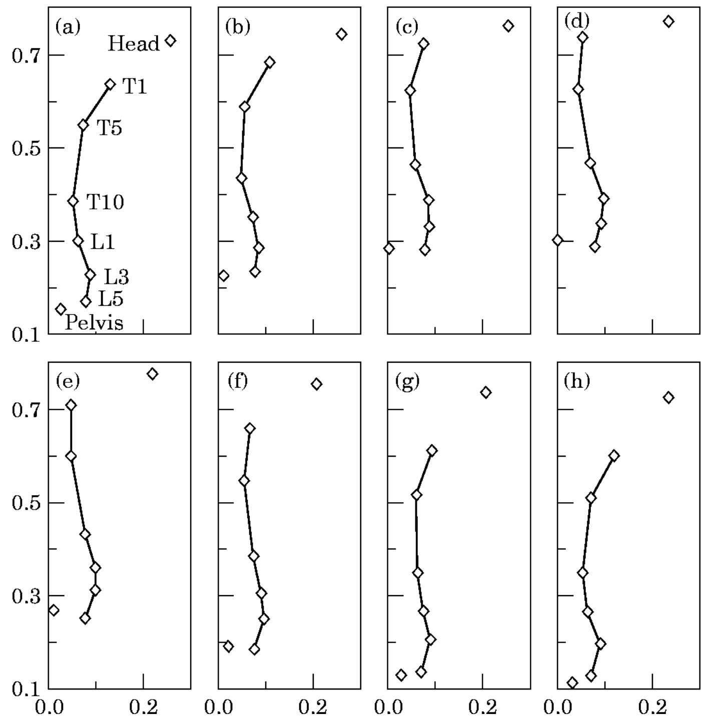

Figure 9. Movement of the upper-body at the principal resonance frequency of the apparent mass of subject 5 at 5·0 Hz. (The units of both axes are metres (m). The scale of the movement is exaggerated for clarity).

5. DISCUSSION

This study indicates that a combination of bending and rocking motions of the spine are involved in the principal resonance of the apparent mass of seated people. Bending of the spine has been suggested in some previous studies. Sandover and Dupuis [6] suggested that the resonances observed during human response to vibration were related to bending in the lumbar spine and possibly a rocking motion of the pelvis. The vertical, fore-and-aft, and angular (pitch) motions at the centroid of T12, L2 and L4 were resolved, and demonstrated resonant behaviour at about 4 Hz. However, the cinematographic technique was found to have insufficient accuracy to measure relative vertical motion between adjacent vertebrae at around the resonance frequency. The measured angular motion, and the calculated relative angular motion between adjacent vertebrae which were greatest at the lower lumbar spine, supported their hypothesis. This is consistent with the present study in which the transmissibility from the seat vertical vibration to pitch motion at L5 was the greatest in the lumbar region at the principal resonance frequency ($p < 0{\cdot}05$).

Bending motion of the lumbar spine at 4·5 Hz was also suggested by Hinz *et al*. [5], using measurements on the body surface over the spinous process of L3 and L4 in the vertical direction (parallel with the body surface) and in the fore-and-aft direction (orthogonal to the surface), together with measurements at the head and the acromion. It was stated that the relative vertical accelerations between L3 and L4 found at 4·5 Hz were mainly caused by bending of the spine, based on relative angular motion between adjacent vertebrae of $0{\cdot}6^\circ$ peak-to-peak per 1 ms^{-2} r.m.s. seat vibration at 4·5 Hz as reported by Sandover and Dupuis [6].

Upon assuming that between the measurement points the spine was straight, as in Figures 9 and 10, the relative angular motions between adjacent 'straight' spines at T5,

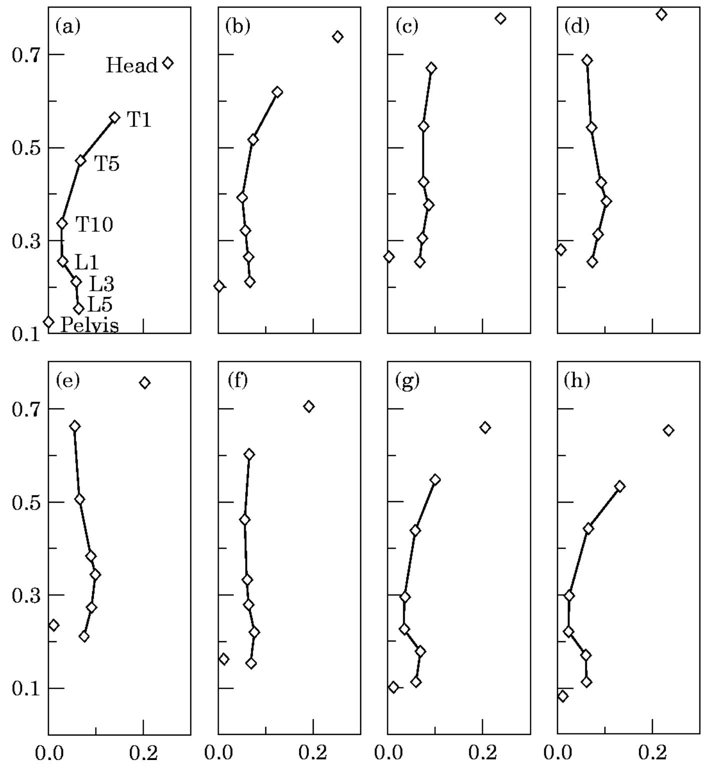

Figure 10. Movement of the upper-body at the principal resonance frequency of the apparent mass of subject 7 at 5·25 Hz. (The units of both axes are metres (m). The scale of the movement is exaggerated for clarity).

T10, L1 and L3 were calculated using simulated time histories for the locations of the ends of each "straight" spine where the motion was measured (see Figure 11). Table 3 shows peak-to-peak relative angular displacements with the sinusoidal seat vibration at the

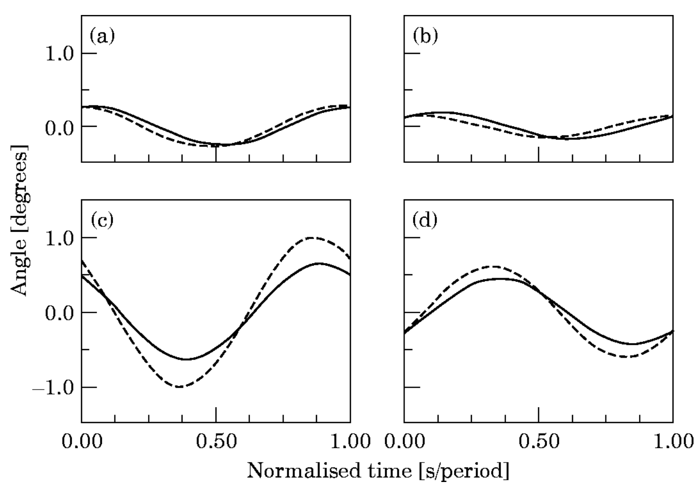

Figure 11. Simulated relative angular motions between adjacent "straight" spines at T5, T10, L1 and L3 for subjects 5 and 7 whose movement of the upper-body is shown in Figures 9 and 10. (With sinusoidal seat vibration at the resonance frequency of the apparent mass at a magnitude of 1·0 ms^{-2} r.m.s.): (a) T5; (b) T10; (c) L1; (d) L3. Key: ——, subject 5; - - - -, subject 7.

TABLE 3

Simulated peak-to-peak relative angular displacements between adjacent "straight" spines at the resonance frequency of the apparent mass with sinusoidal seat acceleration of 1·0 ms^{-2} *r.m.s.* (*the phases were obtained by the time lag between the maximum seat displacement and the relative angular motion*; *in degrees*)

	T5		T10		L1		L3	
Subject	angle	phase	angle	phase	angle	phase	angle	phase
1	0·49	−5	1·33	−134	0·81	18	1·16	−129
2	0·19	−28	0·79	−102	0·41	−96	0·59	98
3	0·27	−92	0·41	−28	1·80	−127	1·43	50
4	0·06	84	1·03	−42	1·23	−161	0·99	27
5	0·52	−83	0·34	−45	1·27	−131	0·89	37
6	0·53	−62	0·86	−95	0·75	170	1·15	21
7	0·55	−99	0·29	−76	2·01	−137	1·22	27
8	0·38	−114	0·52	−102	1·06	−156	0·90	3

resonance frequency of the apparent mass at a magnitude of 1·0 ms^{-2} r.m.s. The phases with respect to the seat vibration were also obtained from the time lag between maximum displacement in the seat vibration and the relative angular motion. The magnitude of the calculated relative angular motions coincided with those reported by Sandover and Dupuis [6] but were slightly larger than those reported by Pope *et al*. [17] who measured the intervertebral motion either between L3 and L4 or between L4 and L5 by means of a device with extensometers, called an intervertebral motion device, mounted skeletally. The values obtained in the lumbar region in this study could be considered as approximations to the relative angular motion between two vertebrae which are adjacent to the vertebra where the motion was measured: the calculated relative angular motion at L1 was that between T12 and L2 which may have been mainly caused by bending of the spine. However, the values reported in the previous studies were obtained from two adjacent vertebrae and could include individual pitch motion of the vertebral bodies which did not result from bending of the spine. The relative angular motion tended to be greatest at L1, although variability between subjects was found. The relative angular motion at L1 was almost out of phase with that at L3, which implies that the spine in this region tended to move in an S-shape. This may be dependent on the initial curvature of the spine.

In Table 3, it is shown that the relative angular motion at T5 was smaller than at the other positions on the lower spine ($p < 0·05$), which implies that bending motion of the upper thoracic spine was less significant than that in the lower spine, as seen in Figures 9 and 10. It is likely that, at the resonance frequency, rocking about a point on the lower thoracic spine was dominant. The rib cage connected to the thoracic spine in this region may restrict bending motion. The rocking of the upper thoracic spine coupled with the bending of the lumbar spine may cause the maximum fore-and-aft transmissibility at T1, at the resonance frequency for all subjects, as shown in Appendix 2.

Kitazaki and Griffin [9, 10] found bending modes of the spine at frequencies close to the principal resonance frequency, although it was concluded that there was no main contribution of any bending motion of the spine to the principal resonance. In their experimental study [9], it was found that a bending mode of the upper thoracic spine and the cervical spine was contained in the fourth mode at 4·9 Hz which was close to the principal resonance frequency. The fifth mode at 5·6 Hz was found to consist of a bending mode of the lumbar spine and lower thoracic spine and a pitching mode of the head. A bending mode of the entire spine was extracted in the fifth mode of their mathematical model at 5·77 Hz [10]. The fourth mode at 5·06 Hz also seemed to contain a bending mode of the lower thoracic spine, although it was not stated. The nature of heavy damping of the human body makes it difficult to determine the extent of the contributions of each vibration mode to the principal resonance, especially when the modes are closely located as in the case of these studies: heavy damping tends to cause closely located modes to couple with each other. In addition, it is usually difficult to determine the damping properties of mechanical systems and there is no reliable data on the damping properties of the human body segments. The bending modes of the spine which were found at frequencies close to the principal resonance in those studies [9, 10] may therefore have made some contribution to the principal resonance.

It seems that a pitching motion of the pelvis occurred together with bending of the lumbar spine at the resonance frequency. Pope *et al*. [4] measured the vertical motion of L3 with an accelerometer attached to a *K*-wire threaded into the spinous process while controlling subjects' posture and muscle tension, together with a pelvis support. The transmissibility to L3 showed a marked peak at 5 Hz, coupled with an attenuation at about 8 Hz, in a reference posture (relaxed), which was altered by changes in the experimental conditions so as to affect "the behaviour of the biological vertical spring and damper system between the pelvis and the seat". This supported their suggestion that "the first natural frequency was due to the biological subsystems between the L3 level and the seat". They also reported that the rotational responses of the pelvis and of the head were likely to be more dominant at about 8 Hz.

Mansfield and Griffin [16] measured the rotation of the pelvis in nine postures and demonstrated that the transmissibilities between seat vertical motion and pelvis pitch rotation were greatest in the frequency range from 10–18 Hz. No significant differences in the transmissibilities between the seat vertical vibration and the pelvis rotation were found in the 4–7 Hz frequency range among the different postures. It was concluded that the pelvis rotation did not contribute to previously reported changes in the 5 Hz apparent mass resonance frequency caused by postural changes.

In the present study, the transmissibility from the vertical seat vibration to the pelvis pitch vibration increased as the frequency increased: six subjects showed a local peak at frequencies between 5·75 and 7·25 Hz, which were higher than the principal resonance frequency of their apparent mass. The main peak might be located at higher frequencies as reported by Mansfield and Griffin [16]. The transmissibility from the seat vertical vibration to the pelvis pitch vibration at the principal resonance frequency of the apparent mass tended to be greater than that to the pitch motion of L5; the difference was found to be statistically significant ($p < 0{\cdot}05$) when excluding one subject who showed a different trend in the upper body movement from the others. However, the difference in the phases of the pitch transmissibilities to the pelvis and to L5 at this frequency was not significant, although the pelvis pitch was expected to be ahead of the pitch of L5 if the pelvis pitch caused the bending of the lumbar spine. Therefore, it was not clear whether the pitch of the pelvis was a cause of the lumbar spine bending or a secondary effect, although the local resonance of the pelvis in pitch occurred at a consistently higher frequency than the resonance frequency of the apparent mass.

Kitazaki and Griffin [9, 10] found a rotational mode of the pelvis with a second visceral mode in their sixth and seventh modes at about 8 Hz, which might have contributed to the second principal resonance in the driving point response. Possibly, a rotational mode of the pelvis may make a minor contribution to the principal resonance at about 5 Hz if there is heavy damping on the mode, as with bending modes of the spine as suggested above.

Kitazaki and Griffin [9, 10] also pointed out the axial and shear deformation of the tissue beneath the pelvis may contribute to the resonance of the apparent mass at about 5 Hz, and this may explain the shift of the resonance frequency due to postural change. The vertical transmissibility to L5 and to the pelvis at the resonance frequency found in this study would be consistent with some local dynamic mechanism between the seat and the level of L5 and the iliac crest. Possibly, the tissue beneath the pelvis contributed the increased motion at the lower part of the upper-body and, consequently, the resonance of the apparent mass. The fore-and-aft motion at L5 at this frequency was small in spite of the pitch of the pelvis, as seen in Figures 9 and 10. It might be hypothesised that at the resonance frequency the pelvis slides backward during forward pitch motion, with deformation of the tissue beneath, and moves foward during backward pitch motion, so as to leave the fore-and-aft motion at L5 small.

From Figures 9 and 10 and the results from the other subjects, it is concluded that any pure axial motions along the spine were not dominant at the resonance frequency, as stated by Kitazaki and Griffin [9, 10], although slight compression and expansion between measurement points on the spine can be seen in Figures 9 and 10. Table 4 shows peak-to-peak relative motions between adjacent measurement points on the spine, calculated using simulated time histories for the measurement locations. The measurements have been divided by the number of intervertebral discs between adjacent measurement points so as to indicate the approximate change in the distance between the centres of adjacent vertebral bodies. A sinusoidal seat vibration at the resonance frequency with a magnitude of 1·0 ms^{-2} r.m.s. was used in the calculation (i.e., a peak-to-peak displacement of approximately 2·9 mm). All calculated values were below 0·4 mm peak-to-peak, except one which appeared to be much greater than the others. Although the variability between subjects and between measurement locations was large, the order of the simulated values was consistent with experimental data reported by Pope *et al*. [17] which also show variability. Pure axial motions along the spine were found to be greater at higher frequencies, although the data are not shown here. It can be hypothesised that the dynamic response of the motion segments of the spine at the resonance frequency consisted of coupled translational and rotational motion in the sagittal plane, as Hinz *et al*. [8] and Pope *et al*. [17] concluded. It is likely, however, that rotational motion is more dominant at this frequency such that coupled bending and rocking of the spine might be more significant as seen in Figures 9 and 10. The two initial curvatures of the spine, and the

TABLE 4

Simulated peak-to-peak relative displacements between adjacent measurement points on the spine divided by the number of intervertebral discs between adjacent measurement points (a sinusoidal seat vibration at the principal resonance frequency with an acceleration of 1·0 ms^{-2} *r.m.s. was assumed; in millimetres, mm)*

Subject	T1–T5	T5–T10	T10–L1	L1–L3	L3–L5
1	0·114	0·006	0·170	0·159	0·148
2	0·097	0·112	0·021	0·064	0·859
3	0·039	0·059	0·134	0·192	0·277
4	0·188	0·155	0·205	0·126	0·026
5	0·026	0·081	0·092	0·336	0·379
6	0·245	0·179	0·096	0·230	0·187
7	0·237	0·148	0·308	0·130	0·220
8	0·215	0·063	0·166	0·377	0·239

eccentricity of the weight of the upper-body with respect to the main vibration transmission path of the body in the vertical direction, may contribute to those dynamic mechanisms of the spine.

The movements of the upper-body of a seated subject at the principal resonance frequency in the apparent mass, as illustrated in this study, may be associated with more than one vibration mode. It might be hypothesised that, at the principal resonance frequency, a bending mode of the spine, a rocking mode of the thoracic spine, a mode involving axial and shear deformation of the tissue beneath the pelvis, and a pitch mode of the pelvis are coupled with each other due to the heavy damping properties of the human body. As Kitazaki and Griffin [9, 10] found, the mode of the viscera, which could be coupled with spinal motion, might also contribute to the resonance, although the motion of the viscera was not measured in this study.

6. CONCLUSIONS

Movements of the seated human body at the principal resonance frequency of the driving-point apparent mass during exposure to vertical seat vibration have been determined using multi-axis transmissibilities to eight locations on the body. The body movements involved translation and rotation within the sagittal plane of the body. The lumbar spine, and probably the lower thoracic spine, tended to bend such that the maximum translational motion caused by the bending occurred in the region around L1, where the spine may deform in an S-shape. The thoracic spine tended to rock about the lower thoracic spine with slight bending along the full length of the thoracic spine; both of these motions were coupled with the bending motion of the lower spine. Pitch motion of the pelvis, which may be accompanied by axial and shear deformation of the tissue beneath the pelvis, also occurred at the resonance frequency, although the pitch resonance of the pelvis occurred at higher frequencies. Any axial motions along the spine were not dominant at the principal resonance frequency near to 5 Hz.

It is hypothesized that more than one vibration mode may contribute to the principal resonance in the apparent mass observed at about 5 Hz. A bending mode of the spine, a rocking mode of the thoracic spine, a mode involving axial and shear deformation of the tissue beneath the pelvis, and a pitch mode of the pelvis may be coupled with each other due to the heavy damping of the human body.

REFERENCES

1. R. R. Coermann 1962 *Human Factors* **4**, 227–253. The mechanical impedance of the human body in sitting and standing positions at low frequencies.
2. T. E. Fairley and M. J. Griffin 1989 *Journal of Biomechanics* **22**, 81–94. The apparent mass of the seated human body; vertical vibration.
3. M. M. Panjabi, G. B. J. Anderson, L. Jorneus, E. Hult and L. Mattsson 1986 *Journal of Bone and Joint Surgery*, *Incorporated* **68A**, 695–702. *In vivo* measurements of spinal column vibrations.
4. M. H. Pope, H. Broman and T. Hansson 1990 *Journal of Spinal Disorders* **3**, 135–142. Factors affecting the dynamic response of the seated subject.
5. F.-W. Hagena, C. J. Wirth, J. Piehler, W. Plitz, G. O. Hofmann and Th. Zwingers 1985 *AGARD Conference Proceedings* **378**, 1–12. *In vivo* experiments on the response of the human spine to sinusoidal Gz-vibration.
6. J. Sandover and H. Dupuis 1987 *Ergonomics* **30**, 975–985. A reanalysis of spinal motion during vibration.

7. W. CHRIST and H. DUPUIS 1966 *International Zeitschrift angewandte Physiologie einschliesslich Arbeitsphysiologie* **22**, 258–278. Über die Beanspruchung der Wirbelsaule unter dem Einfluss sinusformiger und stochastischer Schwingungen.
8. B. HINZ, H. SEIDEL, D. BRÄUER, G. MENZEL, R. BLÜTHNER and U. ERDMANN 1988 *Clinical Biomechanics* **3**, 241–248. Bidimensional accelerations of lumbar vertebrae and estimation of internal spinal load during sinusoidal vertical whole-body vibration: a pilot study.
9. S. KITAZAKI and M. J. GRIFFIN 1998 *Journal of Biomechanics* **31,** 143–149. Resonance behaviour of the seated human body and effects of posture.
10. S. KITAZAKI and M. J. GRIFFIN 1987 *Journal of Sound and Vibration* **200**, 83–103. A modal analysis of whole-body vertical vibration, using a finite element model of the human body.
11. G. S. PADDAN and M. J. GRIFFIN 1988 *Journal of Biomechanics* **21**, 191–197. The transmission of translational seat vibration to the head—I. vertical seat vibration.
12. M. H. POPE, M. SVENSSON, H. BROMAN and G. ANDERSSON 1986 *Journal of Biomechanics* **19**, 675–677. Mounting of the transducers in measurement of segmental motion of the spine.
13. S. KITAZAKI and M. J. GRIFFIN 1995 *Journal of Biomechanics* **28**, 885–890. A data correction method for surface measurement of vibration on the human body.
14. INTERNATIONAL ORGANIZATION FOR STANDARDIZATION 1978 *ISO* 2631. Guide to the evaluation of human exposure to whole-body mechanical vibration and shock.
15. M. MAGNUSSON, M. POPE, M. ROSTEDT and T. HANSSON 1993 *Clinical Biomechanics* **8**, 5–12. Effect of backrest inclination on the transmission of vertical vibrations through the lumbar spine.
16. N. J. MANSFIELD and M. J. GRIFFIN 1997 *Proceedings of Annual Conference of the Ergonomics Society*, 147–152. Effect of sitting posture on pelvis rotation during whole-body vertical vibration.
17. M. H. POPE, A. M. KAIGLE, M. MAGNUSSON, H. BROMAN and T. HANSSON 1991 *Proceedings of the Institution of Mechanical Engineering*, *Part H*, *Journal of Engineering in Medicine* **205**, 39–44. Intervertebral motion during vibration.

APPENDIX 1

Location of the head (the mouth), estimated centres of the vertebral bodies and the pelvis (the posterior-superior iliac spine). (The origin of the co-ordinate system was taken at the seat surface, vertically below the body surface over L5 on the vertical middle line of the back. The y-component (in the lateral axis) was zero for all measurement points, apart from the pelvis which was $-0{\cdot}05$ for all subjects).

(m)	Subject 1, (x, z)	Subject 2, (x, z)	Subject 3, (x, z)	Subject 4, (x, z)
Head	(0·21, 0·72)	(0·27, 0·75)	(0·24, 0·70)	(0·23, 0·78)
T1	(0·080, 0·60)	(0·070, 0·64)	(0·080, 0·62)	(0·080, 0·68)
T5	(0·040, 0·49)	(0·020, 0·51)	(0·040, 0·50)	(0·040, 0·56)
T10	(0·060, 0·34)	(0·035, 0·36)	(0·045, 0·35)	(0·050, 0·42)
L1	(0·075, 0·26)	(0·050, 0·27)	(0·060, 0·28)	(0·065, 0·36)
L3	(0·075, 0·21)	(0·065, 0·21)	(0·065, 0·24)	(0·075, 0·30)
L5	(0·060, 0·15)	(0·060, 0·15)	(0·060, 0·18)	(0·060, 0·23)
Pelvis	(0·0, 0·15)	(0·0, 0·15)	(0·0, 0·18)	(0·0, 0·23)
(m)	Subject 5, (x, z)	Subject 6, (x, z)	Subject 7, (x, z)	Subject 8, (x, z)
Head	(0·22, 0·75)	(0·18, 0·76)	(0·22, 0·72)	(0·17, 0·75)
T1	(0·070, 0·67)	(0·070, 0·66)	(0·090, 0·61)	(0·070, 0·65)
T5	(0·040, 0·57)	(0·030, 0·56)	(0·060, 0·49)	(0·050, 0·55)
T10	(0·045, 0·41)	(0·045, 0·38)	(0·050, 0·36)	(0·045, 0·40)
L1	(0·065, 0·33)	(0·060, 0·32)	(0·055, 0·30)	(0·060, 0·32)
L3	(0·075, 0·27)	(0·070, 0·25)	(0·065, 0·24)	(0·070, 0·26)
L5	(0·060, 0·21)	(0·060, 0·20)	(0·060, 0·18)	(0·060, 0·20)
Pelvis	(0·0, 0·21)	(0·0, 0·20)	(0·0, 0·18)	(0·0, 0·20)

APPENDIX 2

Modulus and phase of the transmissibilities to all measurement points in the vertical and fore-and-aft axes at the principal resonance frequency of the apparent mass.

	Subject 1, 5·25 Hz Vertical		Subject 2, 5·0 Hz Vertical		Subject 3, 5·75 Hz Vertical		Subject 4, 5·25 Hz Vertical	
	Modulus	Phase	Modulus	Phase	Modulus	Phase	Modulus	Phase
Head	1·743	−18·89	0·413	−38·05	1·124	−29·51	1·628	−7·24
T1	1·141	−39·23	1·315	−41·39	1·466	−43·32	1·404	−39·28
T5	1·176	−19·83	1·046	−31·99	1·375	−33·60	1·194	−24·55
T10	1·223	−24·42	1·197	−25·59	1·479	−30·36	1·427	−19·25
L1	1·315	−21·71	1·206	−23·93	1·368	−27·30	1·599	−25·13
L3	1·415	−24·66	1·224	−22·78	1·342	−33·62	1·449	−26·50
L5	1·636	−26·06	1·242	5·30	1·563	−29·09	1·430	−27·19
Pelvis	2·037	−32·11	1·155	−11·11	1·931	−41·16	1·704	−30·04
	Fore-and-aft		Fore-and-aft		Fore-and-aft		Fore-and-aft	
	Modulus	Phase	Modulus	Phase	Modulus	Phase	Modulus	Phase
Head	0·549	54·10	0·662	76·82	0·561	38·63	0·615	71·70
T1	0·968	53·25	0·947	116·22	0·980	90·91	0·833	28·07
T5	0·415	38·09	0·511	140·45	0·284	95·22	0·352	6·91
T10	0·612	−48·21	0·320	−127·96	0·285	−106·54	0·524	−97·89
L1	0·335	−103·88	0·235	−133·65	0·471	−75·29	0·426	−83·89
L3	0·346	−107·66	0·165	164·75	0·134	−153·55	0·349	−141·17
L5	0·401	176·99	0·191	154·69	0·041	−134·41	0·317	−142·16
Pelvis	0·238	−144·93	0·280	52·32	0·330	−173·27	0·516	174·93
	Subject 5, 5·0 Hz Vertical		Subject 6, 5·75 Hz Vertical		Subject 7, 5·25 Hz Vertical		Subject 8, 4·75 Hz Vertical	
	Modulus	Phase	Modulus	Phase	Modulus	Phase	Modulus	Phase
Head	0·473	−62·91	1·422	−15·57	1·415	−31·56	1·447	−2·67
T1	1·315	−34·85	1·493	−33·38	1·526	−38·40	1·497	−16·84
T5	1·203	−26·38	1·047	−11·84	1·137	−18·23	1·213	−6·22
T10	1·240	−20·46	1·471	−19·24	1·376	−20·48	1·295	−7·04
L1	1·337	−24·47	1·392	−21·31	1·643	−30·30	1·440	−10·85
L3	1·454	−30·10	1·173	−14·69	1·448	−28·59	1·601	−14·72
L5	1·681	−27·39	1·274	−19·76	1·526	−23·10	1·557	−10·29
Pelvis	1·954	−34·96	1·849	−31·86	1·936	−34·78	1·624	−15·70
	Fore-and-aft		Fore-and-aft		Fore-and-aft		Fore-and-aft	
	Modulus	Phase	Modulus	Phase	Modulus	Phase	Modulus	Phase
Head	0·574	42·91	0·284	20·65	0·618	55·52	0·631	87·82
T1	0·822	103·45	0·670	79·78	0·926	95·18	0·634	112·86
T5	0·264	129·83	0·131	116·57	0·170	13·06	0·131	90·13
T10	0·278	−105·95	0·432	−71·45	0·681	−54·67	0·440	−47·27
L1	0·370	−76·58	0·257	−37·87	0·851	−53·19	0·504	−39·32
L3	0·118	−115·72	0·150	173·89	0·303	−79·82	0·203	−51·83
L5	0·042	11·42	0·053	−38·01	0·122	−75·03	0·185	−5·70
Pelvis	0·338	150·26	0·357	−41·88	0·139	−144·36	0·248	−9·41